Engineering the Mechanical Properties of Monolayer Graphene Oxide at the Atomic Level

Rafael A. Soler-Crespo,[†,#] Wei Gao,[†,‡,#] Penghao Xiao,[§] Xiaoding Wei,[†,‡] Jeffrey T. Paci,[∥,⊥] Graeme Henkelman,[§] and Horacio D. Espinosa*[,†,‡]

[†]Theoretical and Applied Mechanics Program, Northwestern University, 2145 Sheridan Road, Evanston, Illinois 60208, United States

[‡]Department of Mechanical Engineering, Northwestern University, 2145 Sheridan Road, Evanston, Illinois 60208, United States

[§]Department of Chemistry and the Institute for Computational Engineering and Sciences, The University of Texas at Austin, Austin, Texas 78712-0165, United States

[∥]Department of Chemistry, Northwestern University, 2145 Sheridan Road, Evanston, Illinois 60208, United States

[⊥]Department of Chemistry, University of Victoria, Victoria, British Columbia V8W 3 V6, Canada

Ⓢ Supporting Information

ABSTRACT: The mechanical properties of graphene oxide (GO) are of great importance for applications in materials engineering. Previous mechanochemical studies of GO typically focused on the influence of the degree of oxidation on the mechanical behavior. In this study, using density functional-based tight binding simulations, validated using density functional theory simulations, we reveal that the deformation and failure of GO are strongly dependent on the relative concentrations of epoxide (−O−) and hydroxyl (−OH) functional groups. Hydroxyl groups cause GO to behave as a brittle material; by contrast, epoxide groups enhance material ductility through a mechanically driven epoxide-to-ether functional group transformation. Moreover, with increasing epoxide group concentration, the strain to failure and toughness of GO significantly increases without sacrificing material strength and stiffness. These findings demonstrate that GO should be treated as a versatile, tunable material that may be engineered by controlling chemical composition, rather than as a single, archetypical material.
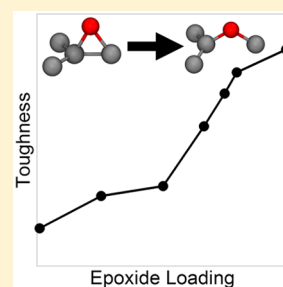
Graphene oxide (GO), an oxygen-functionalized variant of graphene, has recently shown great potential for various applications in sensing,[1−4] energy storage applications,[1,5−7] and the design of advanced composite materials.[1,8−12] While the nanostructure of GO was cause for scientific debate at first, theoretical and experimental evidence available at the time suggested that hydroxyl (−OH) and epoxide (−O−) functional groups dominated the bulk of the material, while carbonyl and carboxylic functional groups preferred to form near free surfaces at the edges of GO flakes.[1,13] Recently, Erickson et al.[14] showed that GO possesses a graphitic backbone stochastically functionalized by functional group clusters, which form island-like patterns, as previously predicted by Lerf and Klinowski.[1,13] It is expected that surface functional groups on GO have considerable influence on the mechanical properties of the material. For instance, monolayer GO was found to have a lower Young's modulus and strength compared to unfunctionalized carbon-based nanomaterials, such as pristine graphene and carbon nanotubes.[15−18] Moreover, it has been shown that both the Young's modulus and strength monotonically decrease as the degree of oxidation increases.[15] As more oxygen atoms become covalently bound to the carbon backbone, the electronic backbone structure becomes dominated by softer, weaker sp^3 bonding. For instance, introducing one epoxide group onto a pristine graphitic backbone would transform two carbons from sp^2 to sp^3 bonding, while the same

effect results from bonding two carbons with a pair of hydroxyl groups. Even though the same degree of oxidation exists in the backbone of GO for both cases, the nature of the functionalization is very different.

An important question, which has not been answered in previous studies, is whether different functionalization affects the mechanical behavior of GO. In fact, due to the complicated nanostructure of GO, experimental and theoretical studies to date report conflicting trends in the observed behavior for GO-based systems.[16,19,20] For instance, Cao et al.[16] reported brittle failure mechanisms observed during membrane deflection experiments, with GO flakes exhibiting a 20% degree of oxidation. Conversely, Wei et al.[20] reported a ductile failure in GO monolayers with a 70% degree of oxidation. Using density functional-based tight binding (DFTB), these authors identified an irreversible epoxide-to-ether bond transformation as the source for ductility. In light of these distinct mechanical behaviors, a more comprehensive investigation that considers the effect of composition of functional groups on GO is required to elucidate the mechanisms that govern its mechanical behavior.
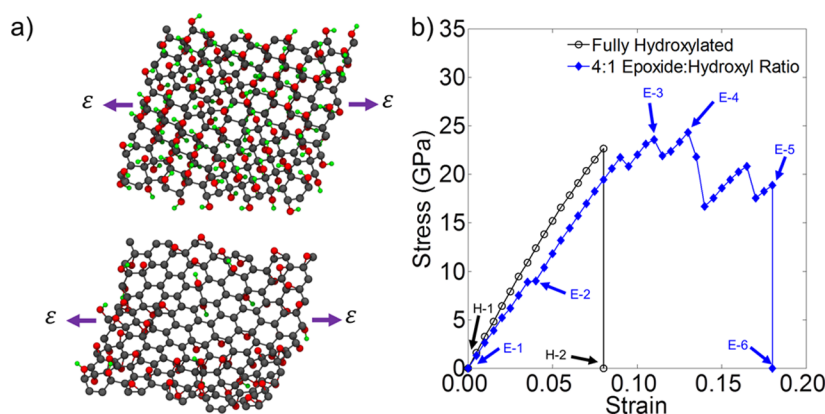
Figure 1. Atomistic configurations and representative stress−strain curves for GO monolayers with different chemical composition. (a) Atomistic models for hydroxyl-rich (top) and epoxide-rich (bottom) GO configurations. Strain (ε) is applied as indicated in the models. Gray, red, and green beads correspond to carbon, oxygen, and hydrogen atoms, respectively. (b) Representative stress−strain curves for hydroxyl- and epoxide-rich GO, tested along the armchair direction. Numbered H and E markers represent atomistic snapshots of interest in Figures 2 and 3, respectively.

In this Letter, we apply atomistic simulations to investigate the interplay between GO chemistry and material deformation. To achieve this, we study extreme cases of GO sheets functionalized purely with epoxide and hydroxyl functional groups, as well as combinations between said functional groups. First, a Monte Carlo-based algorithm[20,21] is employed to generate physical GO models that are both chemically stable and in agreement with previous literature.[15,20−25] Then, we apply the DFTB method (see the Supporting Information for further details) to study the mechanical properties of GO as a function of the composition of functional groups. In particular, the intrinsic atomistic mechanisms that govern material deformation and give rise to the versatility of GO are revealed through a series of comparative calculations. In this way, we identify a multidimensional material design space associated with the chemistry intrinsic to GO during its synthesis, suggesting potential ways to engineer GO with tunable mechanical properties.

Two GO sheets functionalized with representative chemical compositions are considered first (as shown in Figure 1a). The first GO sheet has an epoxide-rich composition. According to previous work,[20] GO synthesized using a modified Hummers's method can reach a 70% degree of oxidation (defined as the fraction of oxidized carbon atoms), with a 4:1 epoxide-to-hydroxyl functional group ratio. For this structure, a small number of carbonyl, oxetane, and ether groups may also be present, consistent with the reports of Erickson et al.[14] using electron microscopy. The second GO sheet considered possesses the same degree of oxidation as that reported by Wei et al. but a hydroxyl-rich composition similar to reports by Cao et al. to highlight the difference in deformation mechanisms due to chemical composition.[16,20] As shown in Figure 1b, we determined the stress−strain curves for the sheets subjected to uniaxial strain along the armchair direction, preventing contraction along the zigzag direction. From these curves, we obtained the Young's modulus (i.e., the slope of the linear elastic regime), strength (i.e., maximum stress), and toughness (i.e., the area under the stress−strain curve up to failure), as discussed in the Supporting Information. The generality of our findings is further discussed in the Supporting Information.

It is interesting to note that after applying a small strain (i.e., bottom left of Figure 1b), the stress−strain responses of the two sheets are similar. Deviations from linear elasticity occur for

the epoxide-rich GO at approximately 4% strain. Moreover, while the maximum load that the material can bear for both compositions is similar (24.3 GPa for epoxide-rich and 22.7 GPa for hydroxylated), the postpeak stress behavior and failure mechanisms are starkly different. Hydroxyl-rich GO undergoes a sudden, brittle failure near maximum load, while epoxide-rich GO withstands significant additional deformation before its eventual failure. This suggests that epoxide groups enable a mechanism that enhances material ductility compared to hydroxyl-rich GO. To understand this effect, we investigate atomistic configurations throughout the deformation process. As shown in Figure 2, failure in hydroxyl-rich structures occurs
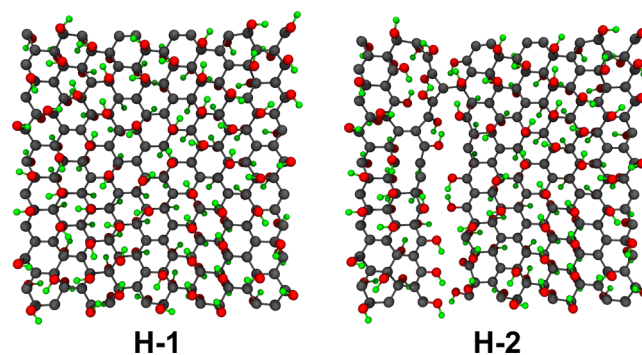

Figure 2. Atomistic configurations of hydroxyl-rich GO during the deformation process. Numbered H markers represent atomistic snapshots of interest, as shown in Figure 1. Gray, red, and green beads correspond to carbon, oxygen, and hydrogen atoms, respectively.

due to the formation of a crack, which propagates abruptly through bonds associated with hydroxyl-functionalized carbon atoms. During failure, hydroxyl groups present along the crack front align with the in-plane direction, as captured in snapshot H-2 of Figure 2. During the crack propagation process, as groups present near the crack tip align with the in-plane direction, repulsions from steric effects manifest in the crack tip, leading to unstable crack growth. Thus, crack propagation mechanisms present when hydroxyl groups are dominant in GO lead to a brittle and catastrophic failure, as observed in experiments reported previously by Cao et al.[16]
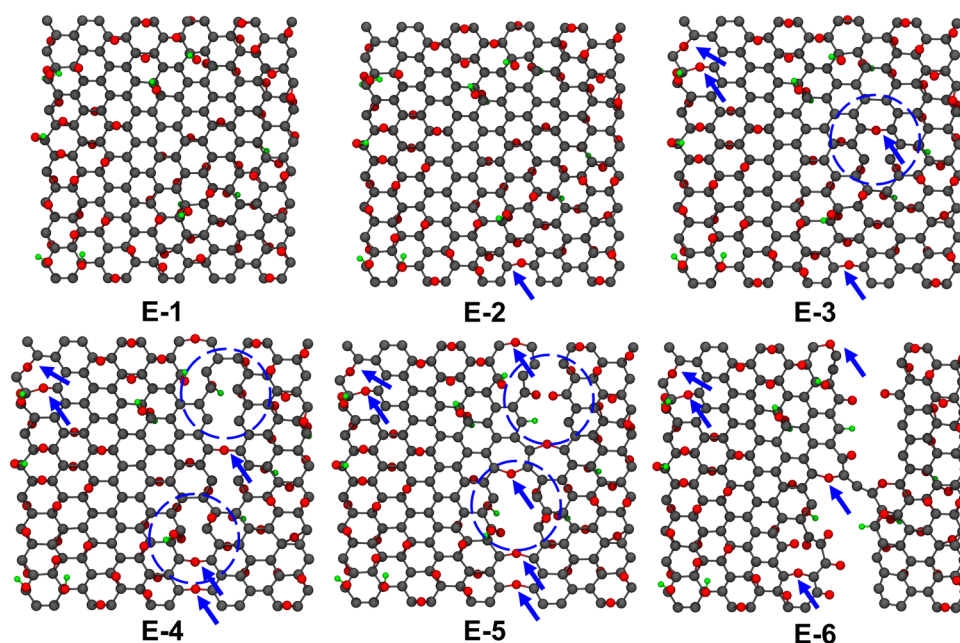
Figure 3. Atomistic configurations of epoxide-rich GO during the deformation process. Numbered E markers represent atomistic snapshots of interest, as shown in Figure 1. Gray, red, and green beads correspond to carbon, oxygen, and hydrogen atoms, respectively. In snapshots E-2 to E-6, arrows and dashed circles are used to indicate epoxide-to-ether transformation events and crack nucleation zones, respectively.
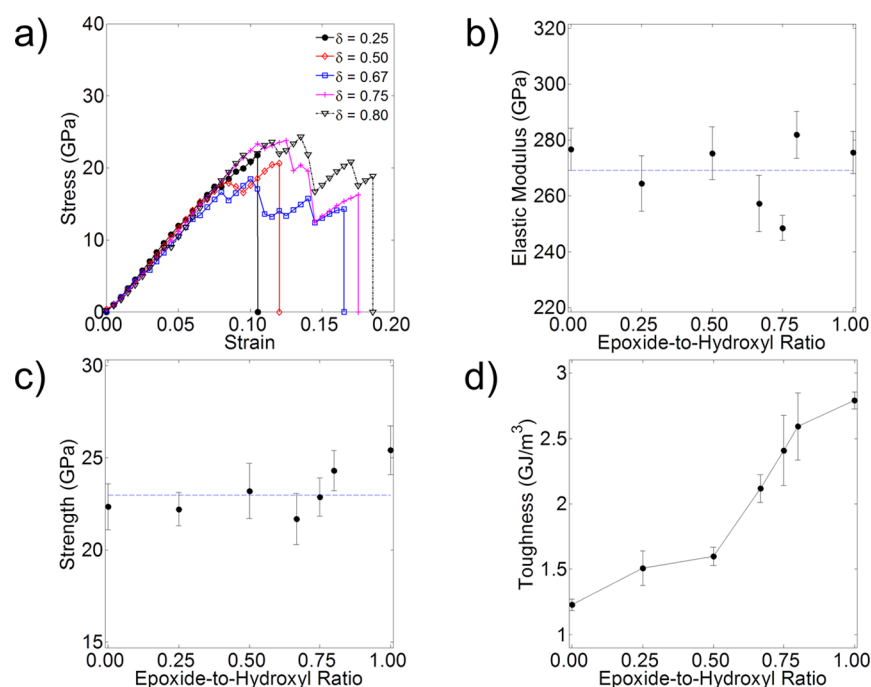

Figure 4. (a) Representative stress–strain curves and the variation of (b) elastic modulus, (c) tensile strength, and (d) toughness for GO sheets with a 70% degree of oxidation and varying epoxide-to-hydroxyl ratios, δ, are shown. All error bars correspond to ±1 standard deviation in material properties obtained from five different structures with random spatial distributions of functional groups.

In contrast to the brittle failure in hydroxyl-rich GO, the epoxide-rich GO exhibits ductile deformation beyond the maximum load. From snapshots E-1 and E-2 in Figure 3, we observe a functional group transformation at 4% strain (marked with a blue arrow), where an epoxide functional group transforms into an ether functional group by cleavage of the C−C bond associated with the epoxide ring, leading to a strain burst shown in Figure 1b. It is important to note that ether groups are covalently bound within the GO sheets and are

more flexible than epoxide rings, allowing GO to bear significantly more deformation than the rest of its graphitic backbone could otherwise achieve. Upon further loading, more epoxide-to-ether transformations take place, as shown in snapshot E-3 in Figure 3. Meanwhile, some sp^3 C−C bonds (not bound within epoxide groups) break in front of the newly formed ether groups, driving the cleavage of the GO sheet through crack propagation, as highlighted in snapshots E-3, E-4, and E-5 in Figure 3, with dashed blue circles indicating crack

nucleation regions. Unlike the case for hydroxyl-rich GO, crack propagation is stabilized due to the energy dissipated through epoxide-to-ether transformations. Moreover, ether groups at the crack tip are highly stretchable due to the flexible C−O−C angles that they form, blunting the crack propagation front and enabling the material to withstand significant deformations before final failure (see snapshot E-6 in Figure 3). These observations clearly suggest that epoxide groups enable GO to exhibit and fail in a ductile fashion, consistent with experimental observations from the epoxide-rich GO studied by Wei et al.[20]

To further elucidate how different compositions of functional groups can affect the mechanical properties of GO, we considered additional configurations that contained a 70% degree of oxidation but differed in terms of chemical composition. We define the ratio of epoxide and hydroxyl groups as

$$\delta = \frac{N_{\text{epoxides}}}{N_{\text{epoxides}} + N_{\text{hydroxyls}}} \tag{1}$$

where N_{epoxides} and $N_{\text{hydroxyls}}$ are the total number of epoxide and hydroxyl groups present in a monolayer. We conducted a series of DFTB calculations on sheets by varying δ from 0 to 1. The stress−strain curves were obtained as before, and representative stress−strain curves are shown in Figure 4a. The stiffness, strength, and toughness of the sheets were calculated as a function of δ and are also plotted in Figure 4.

Interestingly, both the stiffness (Figure 4b) and strength (Figure 4c) of the material are almost independent of the composition. At small deformations, the majority of the load on the sheet is carried by the carbon backbone with negligible load transfer between out-of-plane bonds (i.e., bonds between oxygen and backbone carbon atoms). Although the nature of the functionalization is different in each case, the relative amount of sp²- versus sp³-type C−C bonding remains the same when the oxidation density is kept constant. As a result, the stiffness of the sheet should not be affected by the composition, as shown in previous reports.[15] Furthermore, and because all of the GO sheets shown in Figure 4b,c contain the same degree of oxidation, one should expect the elastic modulus and strength to be approximately constant if (i) the effect of functional groups in the breakdown of the sp² bond network is approximately the same and (ii) spatial distribution effects are negligible. Because one can expect functional groups to degrade the electronic network of graphene through similar mechanisms, this serves as potential validation of the second-order nature of the effects of spatial distribution of functional groups (see the Supporting Information for more details).

The strength of GO corresponds to the peak stress on the stress−strain curves. To understand the effect of composition on strength, we analyzed the nanostructures of GO, where four types of sp³ C−C bond configurations were identified, as shown in Figure 5. The majority of sp³ C−C bonds are type 1 and type 2 in epoxide-rich GO, while type 3 and 4 sp³ C−C bonds become more dominant as the density of epoxide groups (i.e., δ) decreases. Apparently, these sp³ C−C bonds are the "weakest links" in the material from where fracture initiates. The strength of the material is dependent on the maximum loads that these four types of bonds can bear. We build four GO sheets, and each one contains only a single sp³ C−C bond of these four types (see the Supporting Information for more details). The sheets are stretched uniaxially as before, and we record the stress corresponding to the onset of bond breaking
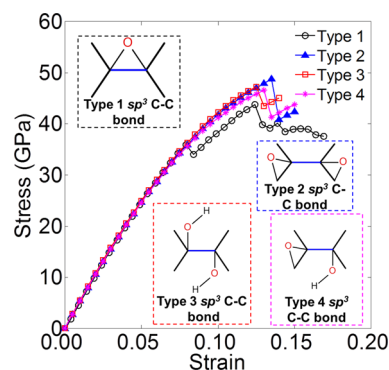

Figure 5. Stress−strain curves for GO sheets containing a single sp³ C−C bond with four different bond types possible in GO.

of these four types. As shown in Figure 5, types 2, 3, and 4 exhibit similar behavior as the stress rises to a similar value before a load drop occurs. For each of these bond types, this load drop corresponds to the sp³ C−C bond breaking followed by unstable crack propagation. By contrast, type 1 sp³ C−C bonds display two load drops. The first drop corresponds to an epoxide-to-ether transformation, beyond which the ether functional group withstands additional load up to a second load drop at stress similar to those in types 2, 3, and 4. The second load drop is due to the stress concentration built up in front of the ether group, which in turn drives the crack propagation. On the basis of the above analysis, the material failure initiated at these four types of sp³ C−C bonds occurs at a similar stress level. Therefore, the strength of GO does not show notable dependence on the composition of functional groups.

To further quantify the degree of ductility introduced by epoxide-to-ether transformations, we studied the toughness (Γ) of GO, which was computed by integrating the stress−strain curve

$$\Gamma = \int_0^{\varepsilon_f} \sigma \, d\varepsilon \tag{2}$$

where ε_f is the ultimate strain upon failure. As shown in Figure 4d, epoxide groups increase the toughness of GO, particularly when δ is above 0.5, allowing the material to absorb energy and deform in a ductile manner before fracturing. The toughening of GO is largely due to the additional material deformation made possible through elastic energy dissipation from epoxide-to-ether transformations and the added flexibility of ether groups. Remarkably, we note that when epoxide content increases, the material becomes more stretchable and ductile without sacrificing its intrinsic strength. This is very interesting because strength and toughness are mutually exclusive for most structural materials.[26] Here, we show the potential for avoiding this trade-off and enhancing material toughness by engineering the chemical composition of GO.

The spatial distribution of functional groups in GO is largely random due to the stochastic oxidation process, as previously shown by Erickson et al.[14] To account for this, five GO structures were generated based on our Monte Carlo algorithm for each oxidation level and composition (i.e., five models with the same degree of oxidation and composition but different spatial distribution were subjected to our simulated mechanical experiments). The randomness in the spatial distribution of functional groups introduced scatter in mechanical properties, as indicated by the error bars in Figure 4. However, the general
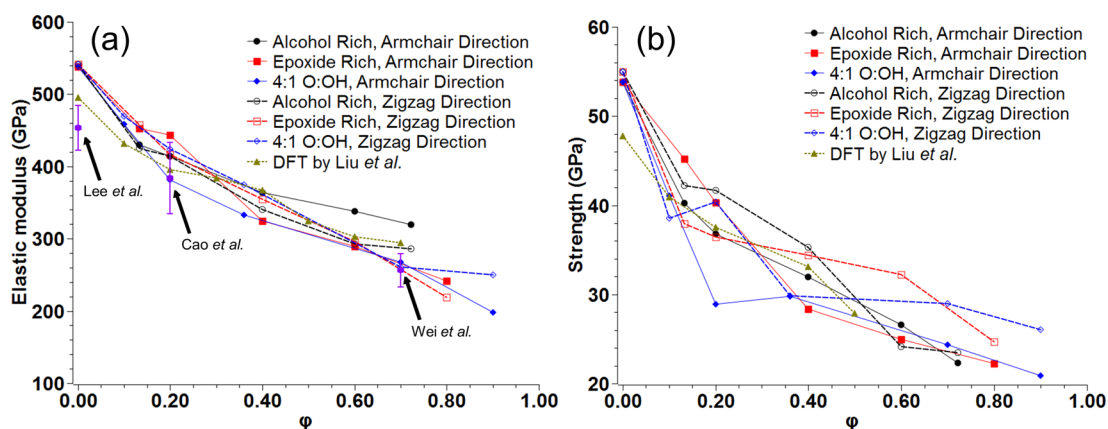
Figure 6. Summary of the (a) elastic modulus and (b) strength for GO sheets with varying epoxide-to-hydroxyl functional group ratio, δ, and degree of oxidation, φ. DFT curves from Liu et al. obtained from ref 15 for amorphous GO are also shown. Error bars correspond to standard deviations from experimental measurements in refs 16, 17, and 20.

trends in the properties do not change as a result of these deviations (see the Supporting Information for further details). The standard deviation of the measurement, when compared to the magnitude of the properties, clearly highlights the fact that spatial distribution indeed acts as a second-order effect in GO. Thus, we took advantage of the relatively high efficiency and accuracy of the DFTB method in order to simulate many GO structures in a reasonable time but recognize that the method is semiempirical. Therefore, we also applied density functional theory (DFT) that has the potential of being more accurate to validate our results, in particular, the epoxide-to-ether group transformation, which we expect plays a critical role in the behavior of different GO structures. The comparison between DFTB and DFT is shown in the Supporting Information. For all of the properties of interest in our study (i.e., Young's modulus, strength, toughness), DFTB shows a consistent stiffening of the system when compared to DFT. However, this is not surprising based on previous reports on carbon nanomaterials that rely on DFTB calculations[27] and the fundamental assumptions made to enhance the computational efficiency of the method.[28] Given the reasonable agreement between DFT and DFTB in terms of mechanical properties and deformation mechanisms observed in the material and the good agreement with experimental findings, we opted to utilize DFTB for our study to benefit from the computational efficiency afforded by the method for the large number of simulations performed in this study.

We also studied the effect of the degree of oxidation on the mechanical properties of GO. Figure 6a,b summarizes the elastic properties and strength of systems simulated in this study when subjected to uniaxial tensile strain along the armchair and zigzag directions, respectively. As reported by both theoretical and experimental investigations of unfunctionalized (i.e., carbon nanotubes and graphene) and functionalized (i.e., GO) carbon nanomaterials, the mechanical properties of functionalized carbon nanomaterials degrade as a function of increasing degree of oxidation.[15−20] Perhaps much more interestingly, from this study, it becomes apparent that elasticity and strength at a certain degree of oxidation are seemingly independent of the composition of the system. This is in agreement with our findings on the effects of the epoxide-to-hydroxyl ratio, δ, where we found that average values of the elastic modulus and strength, at a given degree of oxidation, can capture such properties for a diverse set of GO archetypes.

The results obtained in this Letter suggest the existence of a large design space in which multiple GO properties vary simultaneously as a function of the composition of functional groups. It is shown that epoxide-rich GO outperforms hydroxyl-rich GO, by virtue of increasing toughness without forfeiting strength and stiffness. However, the selection of an "optimal" archetype may be more complicated when other aspects have to be considered. For example, in the application of GO-based nanocomposite materials, the interfacial interactions between stacked sheets are critical to understand composite deformation and failure.[8−12,29,30] It is noted that functional groups without terminal hydrogen atoms require the presence of a chemical "mediator" (e.g., water or polymeric materials) to allow for effective hydrogen-bonding networks to form in the out-of-plane direction.[12,30] Furthermore, the chemical reactions that are accessible to epoxide functional groups are quite limited as compared to hydroxyl functional groups. In this light, the presence of hydroxyl groups may add increased reactivity, opening the door for further chemical changes to occur. While beyond the scope of this work, it is important to understand the role of functional groups in GO interlayer interactions, as well as the interactions between GO and various polymeric materials, which add additional layers of intricacy to the design of the atomistic structure of GO.

In summary, the mechanical properties of GO as a function of chemical composition were studied through a large number of atomistic simulations based on DFTB and selectively validated through DFT studies. It was found that the mechanical behavior of GO strongly depends on the ratio between epoxide and hydroxyl functional groups. Brittle fracture was observed in hydroxyl-rich GO, while epoxide-rich GO favors ductile failure due to a mechanically driven epoxide-to-ether group transformation, enabling GO to absorb energy and prevent failure through crack blunting. Moreover, through this effect, GO exhibits significantly enhanced toughness without loss in material strength and stiffness, in contrast to typical engineering materials. The results highlight the potential to utilize GO as a tunable building block in nanocomposites and many other applications by engineering the chemical composition and, in turn, the mechanical properties of GO monolayers.

ASSOCIATED CONTENT

Supporting Information

The Supporting Information is available free of charge on the ACS Publications website at DOI: 10.1021/acs.jpclett.6b01027.

Computational methods, DFTB methodology validation with DFT, data reduction methods, and supplemental discussion and references (PDF)

AUTHOR INFORMATION

Corresponding Author

*E-mail: espinosa@northwestern.edu.

Author Contributions

#R.A.S.-C. and W.G. contributed equally to this work.

Notes

The authors declare no competing financial interest.

ACKNOWLEDGMENTS

REFERENCES

(1) Dreyer, D. R.; Park, S.; Bielawski, C. W.; Ruoff, R. S. The chemistry of graphene oxide. *Chem. Soc. Rev.* **2010**, *39*, 228−240.

(2) Robinson, J. T.; Perkins, F. K.; Snow, E. S.; Wei, Z.; Sheehan, P. E. Reduced graphene oxide molecular sensors. *Nano Lett.* **2008**, *8*, 3137−3140.

(3) Dua, V.; Surwade, S. P.; Ammu, S.; Agnihotra, S. R.; Jain, S.; Roberts, K. E.; Park, S.; Ruoff, R. S.; Manohar, S. K. All-organic vapor sensor using inkjet-printed reduced graphene oxide. *Angew. Chem., Int. Ed.* **2010**, *49*, 2154−2157.

(4) Ryoo, S.-R.; Lee, J.; Yeo, J.; Na, H.-K.; Kim, Y.-K.; Jang, H.; Lee, J. H.; et al. Quantitative and multiplexed microRNA sensing in living cells based on peptide nucleic acid and nano graphene oxide (PANGO). *ACS Nano* **2013**, *7*, 5882−5891.

(5) Xu, J.; Wang, K.; Zu, S.-Z.; Han, B.-H.; Wei, Z. Hierarchical nanocomposites of polyaniline nanowire arrays on graphene oxide sheets with synergistic effect for energy storage. *ACS Nano* **2010**, *4*, 5019−5026.

(6) Luo, Z.; Vora, P. M.; Mele, E. J.; Johnson, A. C.; Kikkawa, J. M. Photoluminescence and band gap modulation in graphene oxide. *Appl. Phys. Lett.* **2009**, *94*, 111909.

(7) Kuila, T.; Mishra, A. K.; Khanra, P.; Kim, N. H.; Lee, J. H. Recent advances in the efficient reduction of graphene oxide and its application as energy storage electrode materials. *Nanoscale* **2013**, *5*, 52−71.

(8) Xu, Y.; Hong, W.; Bai, H.; Li, C.; Shi, G. Strong and ductile poly(vinyl alcohol)/graphene oxide composite films with a layered structure. *Carbon* **2009**, *47*, 3538−3543.

(9) Medhekar, N. V.; Ramasubramaniam, A.; Ruoff, R. S.; Shenoy, V. B. Hydrogen bond networks in graphene oxide composite paper: structure and mechanical properties. *ACS Nano* **2010**, *4*, 2300−2306.

(10) Beese, A. M.; An, Z.; Sarkar, S.; Nathamgari, S. S. P.; Espinosa, H. D.; Nguyen, S. T. Defect-tolerant nanocomposites through bio-inspired stiffness modulation. *Adv. Funct. Mater.* **2014**, *24*, 2883−2891.

(11) Dikin, D. A.; Stankovich, S.; Zimney, E. J.; Piner, R. D.; Dommett, G. H.; Evmenenko, G.; Nguyen, S. T.; Ruoff, R. S. Preparation and characterization of graphene oxide paper. *Nature* **2007**, *448*, 457−460.

(12) Compton, O. C.; Cranford, S. W.; Putz, K. W.; An, Z.; Brinson, L. C.; Buehler, M. J.; Nguyen, S. T. Tuning the mechanical properties of graphene oxide paper and its associated polymer nanocomposites by controlling cooperative intersheet hydrogen bonding. *ACS Nano* **2012**, *6*, 2008−2019.

(13) Lerf, A.; He, H.; Forster, M.; Klinowski, J. Structure of graphite oxide revisited. *J. Phys. Chem. B* **1998**, *102*, 4477−4482.

(14) Erickson, K.; Erni, R.; Lee, Z.; Alem, N.; Gannett, W.; Zettl, A. Determination of the local chemical structure of graphene oxide and reduced graphene oxide. *Adv. Mater.* **2010**, *22*, 4467−4472.

(15) Liu, L.; Zhang, J.; Zhao, J.; Liu, F. Mechanical properties of graphene oxides. *Nanoscale* **2012**, *4*, 5910−5916.

(16) Cao, C.; Daly, M.; Singh, C. V.; Sun, Y.; Filleter, T. High strength measurement of monolayer graphene oxide. *Carbon* **2015**, *81*, 497−504.

(17) Lee, C.; Wei, X.; Kysar, J. W.; Hone, J. Measurement of the elastic properties and intrinsic strength of monolayer graphene. *Science* **2008**, *321*, 385−388.

(18) Peng, B.; Locascio, M.; Zapol, P.; Li, S.; Mielke, S. L.; Schatz, G. C.; Espinosa, H. D. Measurements of near-ultimate strength for multiwalled carbon nanotubes and irradiation-induced crosslinking improvements. *Nat. Nanotechnol.* **2008**, *3*, 626−631.

(19) Suk, J. W.; Piner, R. D.; An, J.; Ruoff, R. S. Mechanical properties of monolayer graphene oxide. *ACS Nano* **2010**, *4*, 6557−6564.

(20) Wei, X.; Mao, L.; Soler-Crespo, R. A.; Paci, J. T.; Huang, J.; Nguyen, S. T.; Espinosa, H. D. Plasticity and ductility in graphene oxide through a mechanochemically induced damage tolerance mechanism. *Nat. Commun.* **2015**, *6*, 8029.

(21) Paci, J. T.; Belytschko, T.; Schatz, G. C. Computational studies of the structure, behavior upon heating, and mechanical properties of graphite oxide. *J. Phys. Chem. C* **2007**, *111*, 18099−18111.

(22) Lahaye, R.; Jeong, H.; Park, C.; Lee, Y. Density functional theory study of graphite oxide for different oxidation levels. *Phys. Rev. B: Condens. Matter Mater. Phys.* **2009**, *79*, 125435.

(23) Liu, L.; Wang, L.; Gao, J.; Zhao, J.; Gao, X.; Chen, Z. Amorphous structural models for graphene oxides. *Carbon* **2012**, *50*, 1690−1698.

(24) Wang, L.; Sun, Y.; Lee, K.; West, D.; Chen, Z.; Zhao, J.; Zhang, S. Stability of graphene oxide phases from first-principles calculations. *Phys. Rev. B: Condens. Matter Mater. Phys.* **2010**, *82*, 161406.

(25) Yan, J.-A.; Xian, L.; Chou, M. Structural and electronic properties of oxidized graphene. *Phys. Rev. Lett.* **2009**, *103*, 086802.

(26) Wegst, U. G. K.; Bai, H.; Saiz, E.; Tomsia, A. P.; Ritchie, R. O. Bioinspired structural materials. *Nat. Mater.* **2014**, *14*, 23−36.

(27) Zhao, H.; Min, K.; Aluru, N. Size and chirality dependent elastic properties of graphene nanoribbons under uniaxial tension. *Nano Lett.* **2009**, *9*, 3012−3015.

(28) Frauenheim, T.; Seifert, G.; Elstner, M.; Niehaus, T.; Köhler, C.; Amkreutz, M.; Sternberg, M.; Hajnal, Z.; Di Carlo, A.; Suhai, S. Atomistic simulations of complex materials: ground-state and excited-state properties. *J. Phys.: Condens. Matter* **2002**, *14*, 3015−3047.

(29) Liu, Y. L.; Xie, B.; Zhang, Z.; Zheng, Q. S.; Xu, Z. P. Mechanical properties of graphene papers. *J. Mech. Phys. Solids* **2012**, *60*, 591−605.

(30) Roenbeck, M. R.; Furmanchuk, A.; An, Z.; Paci, J. T.; Wei, X.; Nguyen, S. T.; Schatz, G. C.; Espinosa, H. D. Molecular-level engineering of adhesion in carbon nanomaterial interfaces. *Nano Lett.* **2015**, *15*, 4504−4516.